Taylor & Francis
Taylor & Francis Group

RESEARCH PAPER

Check for updates

Matrin-3 acts as a potential biomarker and promotes hepatocellular carcinoma progression by interacting with cell cycle-regulating genes

Hengjing He[a]*, Muhammad Jamal[a]*, Xingruo Zeng[a], Yufei Lei[a], Di Xiao[a], Zimeng Wei[a], Chengjie Zhang[a], Xiaoyu Zhang[a], Shan Pan[b], Qianshan Ding[c], Haiyan Tan[d], Songping Xie[e], and Qiuping Zhang[a,f]

[a]Department of Immunology, School of Basic Medical Sciences, Wuhan University, Wuhan, China; [b]School of Medicine, Wuhan University of Science and Technology, Wuhan, China; [c]School of Medicine, Northwest University, Xian, China; [d]Gastrointestinal Surgery, Renmin Hospital of Wuhan University, Wuhan, China; [e]Department of Thoracic Surgery, Renmin Hospital of Wuhan University, Wuhan, China; [f]Hubei Provincial Key Laboratory of Developmentally Originated Disease, Wuhan University, Wuhan, China

ABSTRACT

Hepatocellular carcinoma (HCC) is one of the leading causes of cancer-related mortality worldwide. The oncogenic role of Matrin-3 (MATR3), an a nuclear matrix protein, in HCC remains largely unknown. Here, we document the biological function of MATR3 in HCC based on integrated bioinformatics analysis and functional studies. According to the TCGA database, MATR3 expression was found to be positively correlated with clinicopathological characteristics in HCC. The receiver operating characteristic (ROC) curve and Kaplan-Meier (KM) curve displayed the diagnostic and prognostic potentials of MATR3 in HCC patients, respectively. Pathway enrichment analysis represented the enrichment of MATR3 in various molecular pathways, including the regulation of the cell cycle. Functional assays in HCC cell lines showed reduced proliferation of cells with stable silencing of MATR3. At the same time, the suppressive effects of MATR3 depletion on HCC development were verified by xenograft tumor experiments. Moreover, MATR3 repression also resulted in cell cycle arrest by modulating the expression of cell cycle-associated genes. In addition, the interaction of MATR3 with cell cycle-regulating factors in HCC cells was further corroborated with co-immunoprecipitation and mass spectrometry (Co-IP/MS). Furthermore, CIBERSORT and TIMER analyses showed an association between MATR3 and immune infiltration in HCC. In general, this study highlights the novel oncogenic function of MATR3 in HCC, which could comprehensively address how aberrant changes in the cell cycle promote HCC development. MATR3 might serve as a prognostic predictor and therapeutic target for HCC patients.

Introduction

Liver cancer remains a global health challenge with increasing incidences worldwide [1]. Hepatocellular carcinoma (HCC) is the major phenotype of liver cancer, accounting for ~ 90% of the overall cases [2]. According to the World Health Organization's statistics for 2020, HCC ranked sixth and third based on morbidity and mortality, with approximately 906,000 new cases and over 830,000 deaths, respectively [3]. The treatment possibilities for HCC consist of decisive therapies such as hepatectomy and liver transplantation. When surgical resection is not a choice, other approaches including chemical, radiofrequency, microwave ablation, or transarterial chemoembolization are used [4,5]. However, these methods are mostly beneficial when performed in early diagnosis. Moreover, the early-stage detection of HCC can improve the five-year survival rate of patients [6]. Unfortunately, majority of HCC cases are diagnosed in advanced stages due to the absence of tumor-specific symptoms in the early stages [7]. Therefore, understanding the molecular mechanism [8] underlying hepatocarcinogenesis and tumor progression is of great significance to improve the early diagnosis and treatment strategies for HCC patients. The last few years have seen the development of novel systemic therapeutic options for HCC. These include the

assessment of immune checkpoint inhibitors (ICIs), either as a single therapy or in combination with other antitumor drugs [9]. However, the heterogeneous tumor immune microenvironment may lead to a distinct therapeutic outcome in patients benefiting from ICIs. Thus, the identification of reliable predictive biochemical factors of response to these ICIs in HCC is critically important [10]. To this end, efforts are needed to explore the role of PD-L1, tumor mutation burden, microsatellite instability, gut microbiota, and other emerging biomarkers [11].

Multiple studies have shown that changes in the composition of the nuclear matrix can lead to changes in nuclear structure, which is considered to be one of the signatures of malignant transformation [12, 13]. In addition, it is reported that nuclear matrix proteins (NMPs) contribute to RNA synthesis, transcription, RNA processing, DNA organization and replication, cell cycle regulation, and DNA repair [14]. In recent years, there has been a growing interest in the investigation of the role of NMPs in carcinogenesis and tumor prognosis [15]. Matrin-3 (MATR3), one of the NMPs, can bind to both DNA and RNA [16, 17]. It is widely involved in a range of processes, including DNA repair [18], nuclear retention of hyper-edited RNAs [19], RNA splicing [20], transcription, and modulating chromatin architecture [21]. Missense mutations in MATR3 have been associated with amyotrophic lateral sclerosis [17]. MATR3 regulates the posttranscriptional regulation of HIV-1 latency [22] and is a Ca^{2+}//calmodulin-binding protein cleaved by caspases [23]. MATR3, as a splicing activator during PDCD1 exon 3 splicing, also plays a crucial role in the production of PD-1 protein and may possibly produce a marked effect on immunotherapy [24]. Downregulation of MATR3 is responsible for reduced proliferation and is a leading cause of endothelial cell necrosis [25]. Moreover, knockdown of MATR3 inhibits cell proliferation, induces cell cycle arrest, and induces cell apoptosis in malignant melanoma cells [26]. MATR3 also plays an important role in enhancing human colorectal cancer and neuroblastoma progression by interacting with long,

non-coding RNA [27, 28]. These findings suggest the oncogenic role of MATR3. However, little is known about the role of MATR3 in HCC.

In this study, integrated computational analysis was performed to check the expression, diagnostic, and prognostic potentials of MATR3 in HCC patients and its association with clinicopathological characteristics in HCC patients. The association between MATR3 expression and immune infiltration was also validated. Functional assays were performed in HCC cells to identify the main interactors of MATR3, which was verified with co-immunoprecipitation and mass spectrometry (Co-IP/MS). Finally, the oncogenic role of MATR3 was further verified in xenograft tumor experiments.

Materials and methods

Expression analysis and survival analysis

The expression matrix and clinical characters of cohorts included the Liver Hepatocellular Carcinoma Project of The Cancer Genome Atlas (TCGA-LIHC), Liver Cancer-RIKEN, Japan Project from the International Cancer Genome Consortium (ICGC-LIRI-JP), and GSE14520 were downloaded from the TCGA (https://portal.gdc.cancer.gov/), ICGC (https://dcc.icgc.org/), and Gene Expression Omnibus (GEO) (https://www.ncbi.nlm.nih.gov/geo/) database, respectively. For the GSE14520 dataset, the probe signal intensity values were transformed by log2. For TCGA-LIHC and ICGC LIRI-JP cohorts, the normalized read counts were transformed by log2. UALCAN (ualcan.path.uab.edu/home) database was used to determine the mRNA level of MATR3 and the relationship between MATR3 and clinicopathological parameters in HCC based on the TCGA database [29]. The microarray dataset GSE14520 was also analyzed for the quantification of the mRNA expression of MATR3 in HCC vs. adjacent normal tissues. The above data from TCGA-LIHC and GSE14520 were then applied to generate receiver operating characteristic (ROC) curves and Kaplan-Meier (KM) curves for exploration of the diagnostic and prognostic value of MATR3 in HCC.

Functional enrichment analysis

The LinkedOmics (http://www.linkedomics.org/login.php) database was applied to find differentially expressed genes correlated with MATR3 based on the TCGA database [30]. The Metascape (http://metascape.org/) database was used for the functional annotation and disease-related enriched analysis of MATR3 co-expressed genes and interacting proteins, such as the Gene Ontology and Kyoto Encyclopedia of Genes and Genomes pathway, DisGeNET, and PaGenBase analysis [31]. The analysis parameters were set as follows: terms with a $p < 0.01$, a minimum count of 3, and an enrichment factor > 1.5. The protein-protein interaction (PPI) network was constructed using the STRING database (https://cn.string-db.org/) and visualized with Cytoscape software [32, 33].

Construction and validation of a two-gene-based prognostic model

TCGA-LIHC cohort was used to construct the prognostic model as the training cohort. Firstly, the relationship between MATR3 and its interacting proteins was determined by the Gene Expression Profiling Interactive Analysis (GEPIA) database (http://gepia.cancer-pku.cn/index.html) [34]. Subsequently, univariate Cox regression analysis and least absolute shrinkage and selection operator (LASSO)-penalized Cox regression analysis were employed to identify the cell cycle-related MATR3-interacting proteins prognostic model in the training dataset. The risk score for each HCC patient was calculated based on the following formula: Risk score $= \Sigma Exp_i * \beta_i$, where Exp_i represents the gene expression of each MATR3-interacting proteins and β_i represents the coefficient of each gene. The median risk score was considered as the cutoff value to divide HCC patients into a high-risk group and a low-risk group. The same formula and cutoff value were applied to the ICGC LIRI-JP cohort for validation. KM analysis, the ROC curve, and area under curve (AUC) were used to judge the prognostic value of the model. Univariate and multivariate Cox analysis were applied to identify whether the model and MATR3 were independent risk factors.

Patients and specimens

The tumor tissues and adjacent normal tissues were obtained from 19 patients who were diagnosed with HCC without any prior radiotherapy or chemotherapy at the Renmin Hospital of Wuhan University (Wuhan, China). All procedures used in this study were compliant with the World Medical Association's Code of Ethics (Declaration of Helsinki) for human experimentation. This study has been approved by the Ethics Committee of Renmin Hospital of Wuhan University, and informed consent was obtained in writing from each patient. The HCC tissue microarray containing 31 carcinoma tissue and paired adjacent tissue was obtained from Shanghai Outdo Biotech (#OD-CT-DgLiv03–002, Shanghai, China). All patients were pathologically diagnosed with HCC.

Immunohistochemistry assay

The HCC tissue and adjacent normal tissue samples were dewaxed in xylene, followed by rehydration with gradient alcohol. Antigen retrieval was completed after heating in citrate buffer (Servicebio Technology, G1202, China). Endogenous peroxidase was blocked with 3% hydrogen peroxide. The tissue microarray slides were incubated with the primary antibody for MATR3 (Abcam, dilution 1:2000, ab151714, UK) at 4°C overnight. Then, tissue microarray slides were washed with phosphate buffered saline (PBS) and incubated with the secondary antibody (Servicebio Technology, G1215, China) for 30 minutes at 37°C. Finally, tissue slides were treated with 3-diaminobenzidine and counterstained with hematoxylin. The histochemistry score (H-score) was calculated to assess the immunohistochemical results. H-score = (percentage of cells of weak intensity × 1) + (percentage of cells of moderate intensity × 2) + (percentage of cells of strong intensity × 3).

Cell culture

HCC cell lines including Bel-7402, HepG2, Huh7, and the human normal hepatic cell line L02 were purchased from the American Type Culture Collection (ATCC) and maintained in Dulbecco's modified Eagle's medium (DMEM, Biological Industries,

Israel) supplemented with 10% fetal bovine serum (FBS, Biological Industries, Israel) and 1% penicillin/streptomycin (Beyotime Biotechnology, China). In addition, the HEK293T cells were obtained from the ATCC and cultured in DMEM containing 10% FBS. Cells were cultured in a 5% CO_2 air incubator at 37°C.

Reverse transcription-quantitative polymerase chain reaction (RT-qPCR)

Total RNA was isolated from patients' tissues and cell lines using the TRIzol reagent (Invitrogen, USA). The mRNAs were reverse transcribed by using HiScript-III RT SuperMix for qPCR (+gDNA wiper) (Vazyme, China) following the manufacturer's protocol. The ChamQ SYBR qPCR Master Mix (Vazyme, China) was used in quantitative RT-PCR analysis with the Quant Studio 6 Flex Real-Time PCR System (Life Technologies, USA). The gene expression levels were normalized with GAPDH and quantified by the comparative Ct ($2^{-\Delta\Delta Ct}$) method. The primer sequences for RT-qPCR are listed in Supplementary Table S1.

Protein extraction and western blot

Cells were washed three times with cold PBS (Beyotime Biotechnology, China) and lysed with RIPA (Beyotime Biotechnology, China) supplemented with the protease inhibitor PMSF (Beyotime Biotechnology, China) on ice for 30 minutes. The concentrations of total protein were measured with the BCA kit (Beyotime Biotechnology, China). The proteins were separated on a 10% SDS-polyacrylamide gel electrophoresis (EpiZyme Biotechnology, China) and transferred to PVDF membranes (Millipore, USA). The membranes were blocked with 5% nonfat milk for 1 hour at room temperature, then incubated with the primary antibodies (Anti-MATR3, Abcam, ab151714, UK; Anti-GAPDH, ABclonal, AC002, USA) overnight at 4°C. After the overnight incubation with the primary antibodies, membranes were washed with TBS-T buffer (Monad, China) six times and incubated with HRP-labeled secondary antibodies (Proteintech, China) for 1 hour. The signals in the membrane were exposed using the ultra-high-sensitivity ECL

kit (MedChemExpress, USA). GAPDH was used as a loading control.

Plasmid construction and infection

The knockdown plasmids of MATR3 and the empty control vector (pPLK/GFP+Puro) were obtained from the Public Protein/Plasmid Library (China). The sequences of short hairpin RNAs (shRNAs) targeting MATR3 were: 5'-GACCTCGCATAACTATCATAA-3' (sh1) and 5'-CCATCAGATAAAGCTGTGAAA-3' (sh2). In addition, the sequence of 5'-GTTCTCCGAACGTGTCACGTT–3' was used as the negative control. The plasmids were co-transfected into HEK293T cells with the packaging plasmids psPAX2 and pMD2.G, which were kindly provided by Dr. Hudan Liu (Frontier Science Center for Immunology and Metabolism, Medical Research Institute, Wuhan University, Wuhan, China). Supernatants containing the lentivirus were collected. For transduction, 3.0×10^5 target cells were incubated with lentiviral supernatant containing polybrene (8 μg/ml) (Santa Cruz, Germany). After 48 hours, the cells were selected in the culture medium containing puromycin. Then, the efficiency of knockdown was validated by RT-qPCR and western blotting.

Cell counting kit-8 (CCK-8) assay

CCK-8 (Dojindo Molecular Technologies, Japan) was used to determine the proliferation ability of HCC cells following the protocol. Briefly, 2.0×10^4/ml cells in 100 μl were seeded in 96-well cell culture plates. 10 μl of CCK-8 solution was added to each well at different time periods (0, 24, 48, and 72 hours) and incubated for 2 hours at 37°C. The absorbance of each well plate was measured at 450 nm.

Colony formation assay

500 cells were added to each well of a 6-well plate and cultured for 12 days to prepare the cells for the colony formation assay. The cultured medium was changed every 4 days. Then, the cells were fixed in 4% formaldehyde, and 0.5% crystal violet solution

was used to stain the cells. Cell colonies were imaged and analyzed.

Flow cytometry analysis

Cell cycle progression was assessed using the cell cycle detection kit (KeyGEN BioTech, Cat. NO: KGA512, China). Cells were resuspended in 500 μl of 70% cold ethanol, fixed for 2 hours and stored at 4°C. The cells were washed with cold PBS and subsequently treated with 50 μl RNase and 450 μl of propidium iodide for 30 min at 4°C before flow cytometry analysis. The cell apoptosis assay was analyzed using Annexin V and 7-AAD kit (BD Biosciences, Cat. NO: 556454, USA) according to the manufacturer's protocol before flow cytometry analysis. The flow cytometer (BD FACSARia™ III; BD Biosciences, USA) and Flow Jo software were applied to detect and analyze the results.

Wound healing assay

5.0×10^5 cells/well were seeded into 6-well plates. After achieving 80%-90% confluence, the cell monolayer was wounded using a sterile 10 μl pipette tip and washed twice with PBS. The gap widths were imaged at 0, 24, and 48 hours after wounding and were measured from the photomicrographs. The percentage of wound closure was evaluated by measuring migration distances (spaces between the black vertical lines).

Transwell assay

Cell migration was measured in the transwell chamber (pore diameter, 8.0 μm, Corning, USA). After shRNA transfection, a total of 3.0×10^4 cells were plated in the upper chamber and cultured in 100 μl medium with 1% FBS. Meanwhile, 600 μl of medium containing 10% FBS was added to the lower chambers. After migrating for 24 hours at 37°C, cells in the lower chambers were fixed with 4% paraformaldehyde and then stained with 0.5% crystal violet solution. In the end, cells from four randomly selected fields were counted under a light microscope.

Co-immunoprecipitation and mass spectrometry (Co-IP/MS)

The cells inoculated in 10 cm² Petri dishes were washed twice with PBS buffer when they reached 80% ~ 90% confluence and then lysed in cell lysis buffer (Beyotime Biotechnology, P0013, China) for 30 min at 4°C. Then, the lysed supernatant was incubated with 5 μg of anti-MATR3 (Abcam, ab281927, UK) and anti-IgG (Abcam, ab18413, UK) for 12 hours, respectively, and the co-immunoprecipitated products acquired by anti-IgG were used as a control group. After that, 50 μl of Protein A/G magnetic beads (MedChemExpress, Cat. No.: HY-K0202, China) were added to each of the samples and then incubated at 4°C on an a rotating device for 4 hours. Two-fifths of the bead mixture was separated by SDS-PAGE, and then the western blot and Coomassie blue staining were applied to evaluate the efficiency of the Co-IP strategy. The remaining three-fifths of the bead mixture was washed three times with cold PBS slightly and then analyzed by liquid chromatography-mass spectrometry assay with the assistance of SpecAlly Life Technology Co., Ltd., Wuhan, China.

Immune infiltration analysis

CIBERSORT was applied to calculate the relative proportion of the 22 immune cells in each HCC sample and evaluate the immune score in HCC samples with high or low MATR3 expression based on the TCGA database [35]. In addition, we used the tumor immune estimation resource (TIMER) database to evaluate the correlation between MATR3 expression and the levels of immune infiltrating cells in HCC, including CD8^{+} T cells, dendritic cells, B cells, CD4^{+} T cells, neutrophils, and macrophages [36]. Moreover, the correlation between MATR3 and immune marker sets was evaluated by TIMER and GEPIA analysis.

Subcutaneous xenograft tumor model in nude mice

For the *in vivo* tumorigenesis assay, BALB/c nude mice (male, 4–6 weeks old, $n = 20$ at the Institute

of Model Animals, Wuhan University, China) were housed and bred in a specific pathogen-free animal facility. The animal care protocol was approved by the Medical Ethics Committee of Wuhan University School of Medicine (Permit Number: WP20220037). Tumor xenografts were established by subcutaneously injecting 100 μl of PBS containing 5.0×10^6 stable transfected HepG2 cells (control or MATR3 knockdown, $n = 5$ per group). The weight and tumor diameter (length and width) of each mouse were measured every three days. The tumor volume was determined using the following calculation: $0.5 \times$ length $\times$ width $\times$ width. Twenty-one days after the inoculation, the mice were euthanized, and the tumors were evaluated and photographed.

Statistical analysis

Statistical analyses were performed using GraphPad Prism software (version 8.0, USA). Paired t-test, unpaired t-test, and one-way analysis of variance (ANOVA) were used. p value < 0.05 was considered to indicate statistical significance.

Results

Upregulation of MATR3 in HCC cells and patient samples

Based on TCGA and GEO databases, we found an elevated mRNA level of MATR3 in HCC as compared to normal liver tissues (Figure 1(a),(b)). Besides, the results of RT-qPCR and immunohisto-chemistry confirmed the increased expression of MATR3 on both mRNA and protein levels in HCC tissues compared to adjacent normal tissues (Figure 1(c)–(e)). Moreover, HCC cell lines, including Huh7, HepG2, and Bel-7402 also displayed increased expression of MATR3 as compared to the normal hepatic cell line L02 by RT-qPCR and western blot (Figure 1(f),(g)). Taken together these results suggest the upregulation of MATR3 in HCC.

Relationship between MATR3 and clinicopathological features of HCC

Despite the high expression of MATR3 observed in HCC, the clinical features of MATR3 in HCC remains largely unknown. The association of MATR3 with clinicopathological parameters was analyzed using the UALCAN database. MATR3 was found to be significantly correlated with the clinical stages of HCC characterized by the increased expression of MATR3 in the advanced stage of the tumor (Figure 2(a)). Similarly, MATR3 expression increased with an increase in the tumor grade (Figure 2(b)). In addition, high MATR3 expression showed a positive association with regional lymph node metastasis (Figure 2(c)). MATR3 also showed a positive association with TP53 mutation status and was significantly over-expressed in HCC patients with TP53 mutations (Figure 2(d)). In short, the expression of MATR3 in HCC patients was significantly correlated with clinicopathological features, such as clinical stage, tumor grade, nodal metastasis, and TP53 mutation status.

Diagnostic and prognostic potential of MATR3 in HCC patients

In addition, the ROC curve was used to explore the diagnostic activity of MATR3 in HCC. MATR3 showed high diagnostic accuracy based on the TCGA dataset with an AUC = 0.874 (95% CI 0.830–0.918; $p < 0.0001$) (Figure 2(e)), and in GSE14520 dataset with an AUC = 0.85 (95% CI 0.814–0.887; $p < 0.0001$) (Figure 2(f)). The KM curve revealed that the elevated MATR3 predicted poor overall survival (OS) in the TCGA dataset ($p = 0.001$) (Figure 2(g)) and GSE14520 dataset ($p = 0.006$) (Figure 2(h)) of HCC patients. These results reveal the diagnostic and prognostic potential of MATR3 in HCC.

Functions and pathways of co-expressed genes of MATR3 in HCC

To gain insight into the biological function of MATR3 in HCC, the function module of LinkedOmics was used to determine the co-expressed genes of MATR3. The positively and negatively correlated genes are represented as red and green dots respectively, on the volcano plot (Supplementary Figure S1a). The top 50 positive and negative genes correlated with MATR3 are displayed as a heatmap (Supplementary Figure
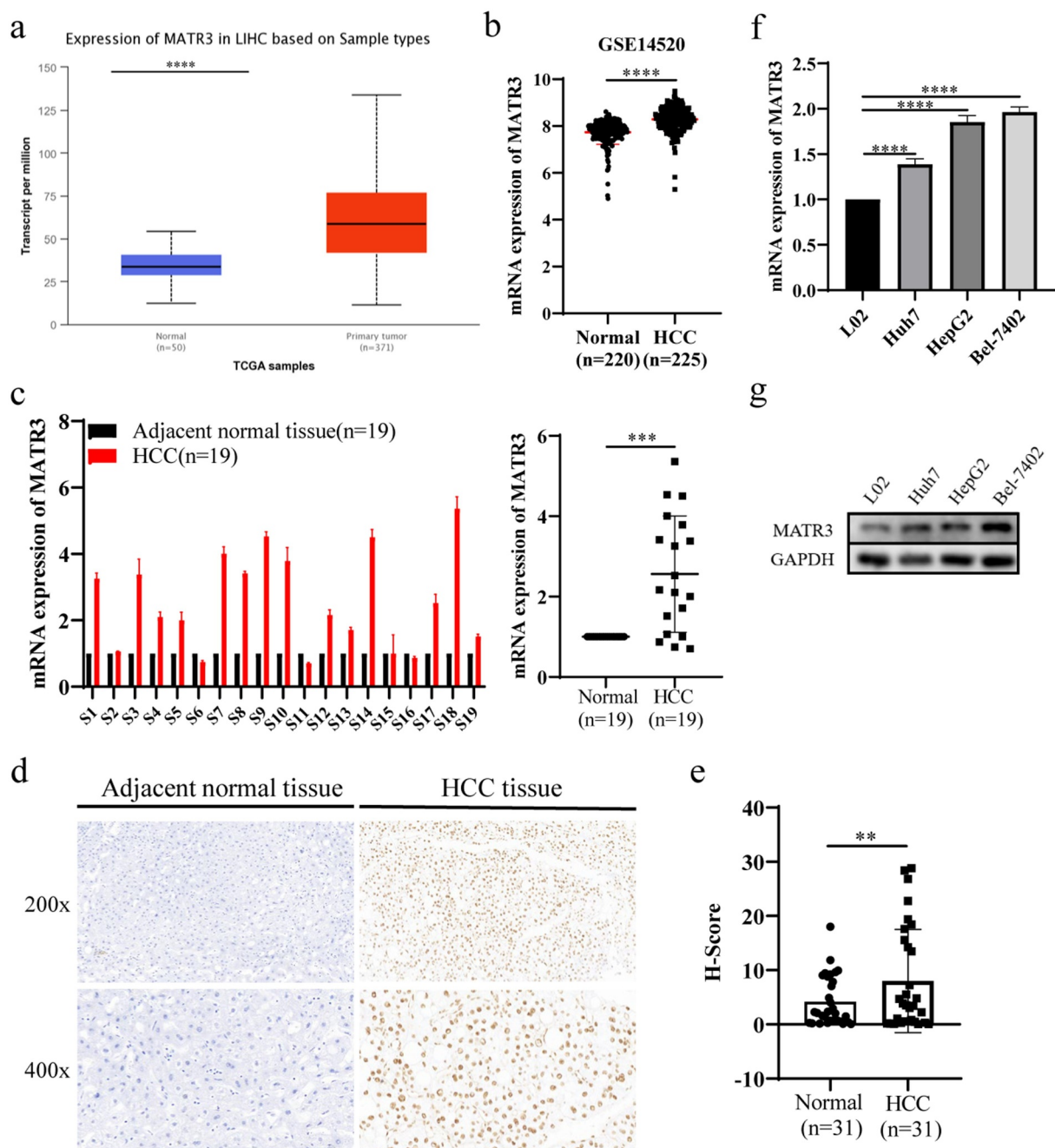
Figure 1. MATR3 is overexpressed in HCC.

(a) UALCAN dataset indicated the mRNA expression of MATR3 in HCC tissues in TCGA database. (b) The mRNA level of MATR3 in HCC tissues in GSE14520 dataset. (c) MATR3 mRNA expression in HCC and adjacent normal tissues were explored by RT-qPCR. (d) Immunohistochemistry images represented MATR3 protein expression in HCC and adjacent normal tissues (magnification, 200×; 400 ×). (e) H-scores of HCC and adjacent normal tissues. (f-g) RT-qPCR and western blot analysis of MATR3 expression in the normal hepatic cell line L02 and three HCC cell lines (HuH7, HepG2 and BEL-7402). ****$p < 0.0001$, ***$p < 0.001$, **$p < 0.01$, *$p < 0.05$, n.s, not significance. HCC, hepatocellular carcinoma. LIHC, liver hepatocellular carcinoma.

S1b). The co-expressed genes with a Pearson correlation greater than 0.6 were selected for enrichment analysis through Metascape. The description of selected genes is listed in supplementary Table S2. The possible pathway enrichment analysis showed the enrichment of MATR3 primarily in the processing of capped intron-containing pre-mRNA, transcription (DNA-templated), mitotic
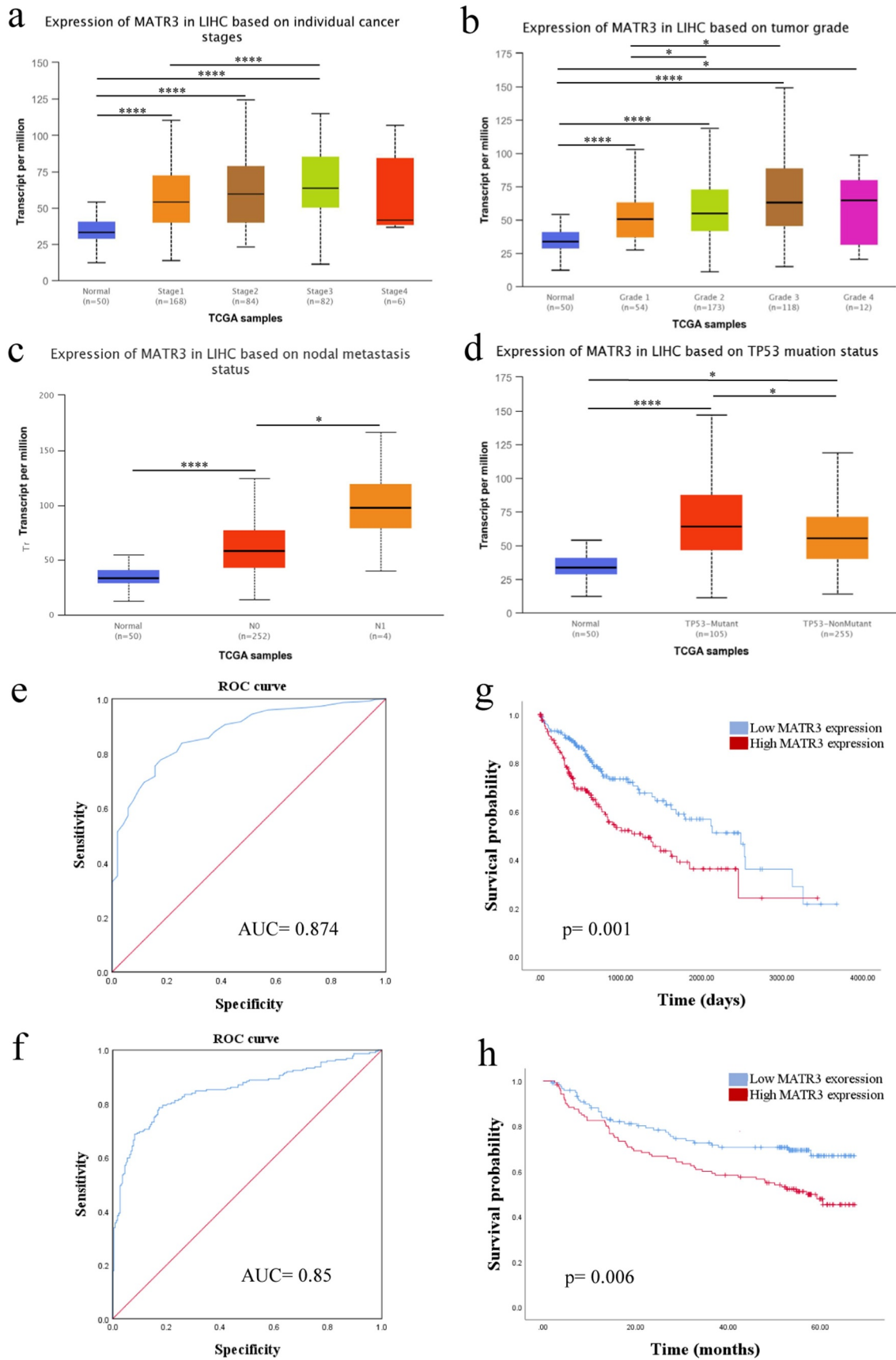
Figure 2. The clinical characteristics of MATR3 high expression in HCC patients.

cell cycle process, cellular response to DNA damage stimulus, and cell cycle (Supplementary Figure S1c).

Knockdown of MATR3 impaired the proliferation and arrested the cell cycle of HCC cells

To explore the potential functions of MATR3 in HCC cells and verify whether MATR3 might affect the cell cycle, HCC cell lines including Bel-7402 and HepG2 cells expressing a relatively high level of MATR3 were transfected with two different shRNAs to repress MATR3 expression. Based on the efficiency of knockdown, the shMATR3–1 was selected for subsequent tests (Figure 3(a),(b)). Firstly, CCK-8 assays were used to evaluate the effect of MATR3 on cell proliferation. Compared with the control group, the OD450 value of the shMATR3 group was significantly lower, indicating that MATR3 positively regulated the proliferation of HCC cells (Figure 3(c),(d)). In addition, the results of colony formation assays demonstrated that the downregulation of MATR3 significantly reduced the colony formation efficiency of HCC cells (Figure 3(e),(f)). All the above results suggest that MATR3 promoted proliferation in the HCC cells. Next, to assess the function of MATR3 in promoting cell proliferation by regulating the cell cycle, we performed flow cytometry analysis. Compared to the control cells, MATR3-depleted cells significantly displayed more sub-G0/G1 cells and fewer sub-S cells (Figure 3(g),(h)), suggesting that inhibition of MATR3 could induce cell cycle arrest. We then investigated expression levels of cell cycle-related markers of shMATR3 and control through RT-qPCR. Compared to the control group, cyclin-dependent kinase 6 (CDK6), cyclin D1 (CCND1), and cyclin D2 (CCND2) mRNA expression was notably downregulated, while that of cyclin-dependent kinase inhibitor p21 (p21) and cyclin-dependent kinase inhibitor p27 (p27) were obviously increased, and those of cyclin-dependent kinase 4 (CDK4) and cyclin E1 (CCNE1) showed no significant difference in shMATR3 transfected cells (Figure 3i, j). These findings indicate that MATR3 may regulate cell cycle, which are in agreement with the results from the enrichment analysis of co-expressed genes of MATR3.

Since apoptosis also has an important effect on cell proliferation [37], we analyzed the effect of MATR3 on cell apoptosis. However, we observed no significant change in apoptosis after silencing MATR3 (Supplementary Figure S2a-b). Next, we examined whether MATR3 had an effect on cell migration in order to corroborate our previous bioinformatics results that the expression of MATR3 was related to metastasis in HCC patients (Figure 1(c)). We performed wound healing and transwell assays. However, we found no remarkable effects of MATR3 silencing on the migration of HCC cells (Supplementary Figure S2c-f). Based on the above findings, we suggest that MATR3 promotes cell proliferation mainly by regulating the expression of cell cycle-associated markers.

The identification of MATR3-interacting proteins and enrichment analysis

To explore the molecular mechanism of MATR3 regulating cell cycle in HCC cell lines, we conducted Co-IP/MS analysis in the Bel-7402 cell line to screen out the protein interactome of MATR3. The black arrow indicates the MATR3 protein (117kDa) and the result of the western blot shows the enrichment of MATR3 was in the mixture in the MATR3 group but not in the control group, indicating the efficiency of the Co-IP strategy in our study (Figure 4(a)). Liquid chromatography-mass spectrometry experiment was applied to identify the MATR3-interacting proteins. An interactome consisting of 179 proteins was detected in the MATR3 group. We then screened out 54 nuclear proteins based on the UniProt database (Supplementary Table S3). Among the candidate proteins, we found PTBP3, SRSF3, SRSF7, STAG2, and PDS5A, were all already known as interaction partners of MATR3, confirming the validity of our investigation [38–40].

(a-d) Association of MATR3 with clinical stage, HCC grade, nodal metastasis and TP53 mutation in HCC patients from UALCAN database. (e-f) The diagnostic significance of MATR3 in HCC patients was accessed by ROC curve based on TCGA and GSE14520 datasets. (g-h) KM analysis predicted the prognostic value of MATR3 in HCC patients based on TCGA and GSE14520 datasets. ****$p < 0.0001$, ***$p < 0.001$, **$p < 0.01$, *$p < 0.05$, n.s, not significance. HCC, hepatocellular carcinoma. LIHC, liver hepatocellular carcinoma. N0, without nodal metastasis. N1, with nodal metastasis. ROC, receiver operating characteristic. KM, Kaplan-Meier. AUC, area under curve.
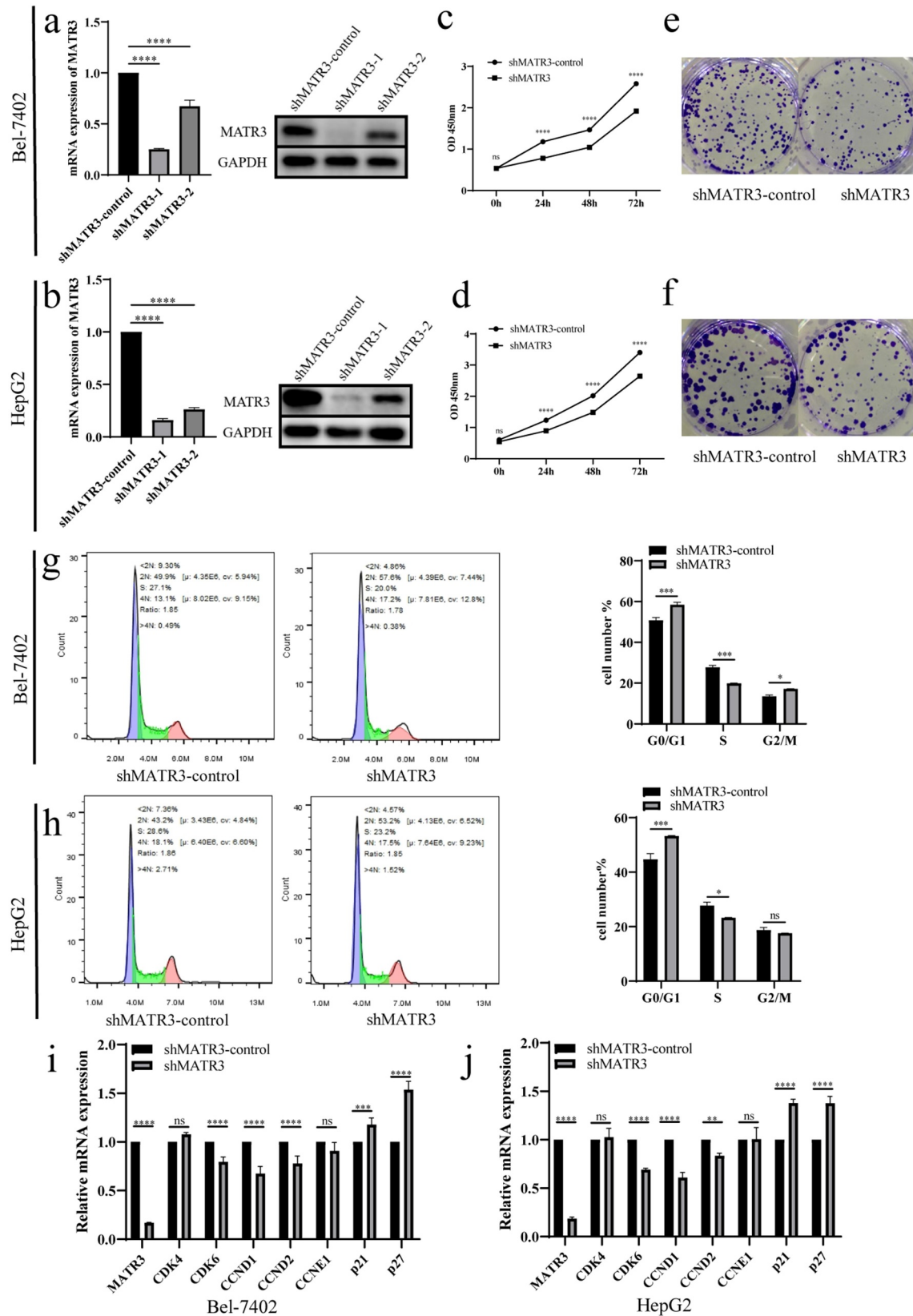
Figure 3. Knockdown of MATR3 arrested cell cycle and inhibited cell proliferation of HCC *in vitro*.

(a-b) RT-qPCR and Western blot verified the efficiency of knocking down MATR3 by shRNA in HCC cell lines, Bel-7402 and HepG2. (c-f) The proliferation of HCC cells indicated by CCK-8 assay and colony formation assay. (g-h) Flow cytometry was used to analyze the impact of MATR3 on cell cycle of HCC cells. (i-j) Knockdown of MATR3 altered expression of cell cycle-related markers. ****$p < 0.0001$, ***$p < 0.001$, **$p < 0.01$, *$p < 0.05$, n.s, not significance.

Figure 4. The identification of MATR3-interacting proteins and enrichment analysis.
(a) The results of Coomassie blue staining and western blot confirmed the efficiency of the Co-IP strategy. The black arrow indicated the MATR3 protein. (b) The main functions of MATR3-interacting proteins were predicted through enrichment analysis. (c) PPI network for MATR3 and its interacting proteins. PPI, protein-protein interaction.

Table 1. The list of MATR3-interacting proteins enriched in cell cycle-related pathways.

GO	Description	Enriched genes
R-HSA-69242	S Phase	CDK2, PRIM2, PSMD5, RAD21, RFC2, RFC5, STAG2, PDS5A, RCC1, PRKCB, TERF2IP, NCAPG, ZNF207, ZNF827, BCCIP, GNL3, DDX6, UBA2, CBX5, CFAP20, GTF2F1
R-HSA-69206	G1/S Transition	CDK2, PRIM2, PSMD5

Pathway enrichment analysis demonstrated that MATR3-interacting proteins expressed in the nucleus were involved in multiple pathways including the metabolism of RNA, S-phase of cell cycle, and the extension of telomeres (Figure 4(b)). We further constructed a PPI network of MATR3 and its interacting proteins in STRING, which was subsequently visualized in Cytoscape that displayed the possible direct and indirect association between MATR3 and its interactome (Figure 4(c)). In line with the computational and cytological experiments, we speculated on the cell cycle-regulating role of MATR3 in HCC along with its interacting proteins. Therefore, we next identified 22 MATR3-interacting proteins in the cell cycle-related pathway (S phase and G1/S transition) (Table 1). Among these proteins, STAG2 and PDS5A have been verified as the interaction partners of MATR3 [40].

Construction and validation of a two-gene-based prognostic model

The prognostic model could provide an important reference for clinicians to identify patients at high risk for poor survival [41,42]. Therefore, we constructed a cell cycle-related prognostic model based on the MATR3 interactome for HCC

patients. Among the cell cycle-related interactors, we found a set of four positively associated genes with MATR3 (Supplementary Figure S3a), of which general transcription factor IIF subunit 1, replication factor C 2 (RFC2), and DNA primase subunit 2 (PRIM2) were positively correlated with the prognosis of HCC patients in the TCGA database by univariate cox analysis (Supplementary Figure S3b). Then these significant genes were subjected to LASSO-Cox regression analysis to construct the prognostic model. The calculation of the regression coefficient was visualized in Supplementary Figure S3c. The prognostic model performed best when two genes were included (Supplementary Figure S3d). The risk score was calculated as follows: $0.1683 * ExpressionRFC2 + 0.3295 * ExpressionPRIM2$. Patients in the training dataset and testing dataset were further divided into a high-risk group and a low-risk group based on the median risk score (Supplementary Figure S3e, h). The KM curve analysis results showed that the low-risk group possessed a better prognosis than the high-risk group in the training dataset (HR = 1.514, 95% CI 1.07–2.142; $p < 0.05$) and testing dataset (HR = 3.024, 95% CI 1.569–5.828; $p < 0.0001$) (Supplementary Figure S3f, i). In addition, the AUC for 3-year OS was 0.627 and 0.754 in the training dataset and testing dataset respectively, implying that the prognostic signature had good accuracy in the prognostic prediction of HCC (Supplementary Figure S3 g, j). Then, the performance of this two-gene model in HCC patients was further assessed with MATR3 and other common prognostic factors by univariate and multivariate Cox regression analysis. Univariate Cox analysis indicated that MATR3 and the model all possessed prognostic effects (all $p < 0.05$) (Supplementary Figure S4a), but multivariate Cox regression analysis showed the opposite results (all $p > 0.05$) (Supplementary Figure S4b). However, when MATR3 and the model were separated and conducted with other factors in multivariate regression analysis respectively, they were all independent prognostic factors (Supplementary Figure S4c-d). Moreover, the statistical significance of MATR3 was greater than the model as an independent prognostic factor in HCC.

The association between MATR3 expression and immune infiltration in HCC

Tumor-infiltrating immune cells (TIICs), as vital factors of the tumor microenvironment, play an important role in the occurrence and development of tumors [43]. Independent tumor-infiltrating lymphocytes play a crucial role in the immune microenvironment and can impact the prognosis of various cancers [44]. It is unclear whether MATR3 has an influence on the recruitment of immune cells and the level of immune infiltration in HCC. Therefore, we first studied the immune infiltration of 22 immune cells in HCC patients using CIBERSORT. The results showed that the proportions of the 22 immune cells varied in different patients (Figure 5(a)). Moreover, CIBERSORT was utilized to evaluate the immune scores in HCC samples with high and low MATR3 expression. The 371 tumor samples were divided into two groups based on MATR3 expression, with 186 samples in the high-expression group and 185 samples in the low-expression group. As shown in Figure 5(b), B cell memory ($p < 0.01$), CD8$^+$ T cells ($p < 0.01$), activated NK cells ($p < 0.01$) and activated mast cells ($p < 0.05$) displayed a dysregulated score with MATR3 expression. We further explored the association between MATR3 expression and TIICs in HCC using TIMER online website. The results demonstrate that MATR3 expression shows a positive correlation with the levels of B cells (correlation = 0.353, $p < 0.0001$), CD8$^+$ T cell (correlation = 0.284, $p < 0.0001$), CD4$^+$ T cell (correlation = 0.398, $p < 0.0001$), macrophages (correlation = 0.456, $p < 0.0001$), neutrophil (correlation = 0.462, $p < 0.0001$), and dendritic cells (correlation = 0.44, $p < 0.0001$) (Figure 5(c)).

To further elucidate the relationship between MATR3 expression and immune infiltration cells, the correlation between MATR3 expression and the diverse marker genes of TIICs was investigated by TIMER analysis. As shown in Table 2, the expression of MATR3 was positively correlated with the major biomarkers of monocyte, tumor-associated macrophages (TAMs), M1 macrophages, M2 macrophages, neutrophils, dendritic cells, and different functional T cells (Th1, Th2, Tfh, Th17, Treg). The GEPIA analysis further confirmed the aforementioned results that MATR3 expression was positively associated with
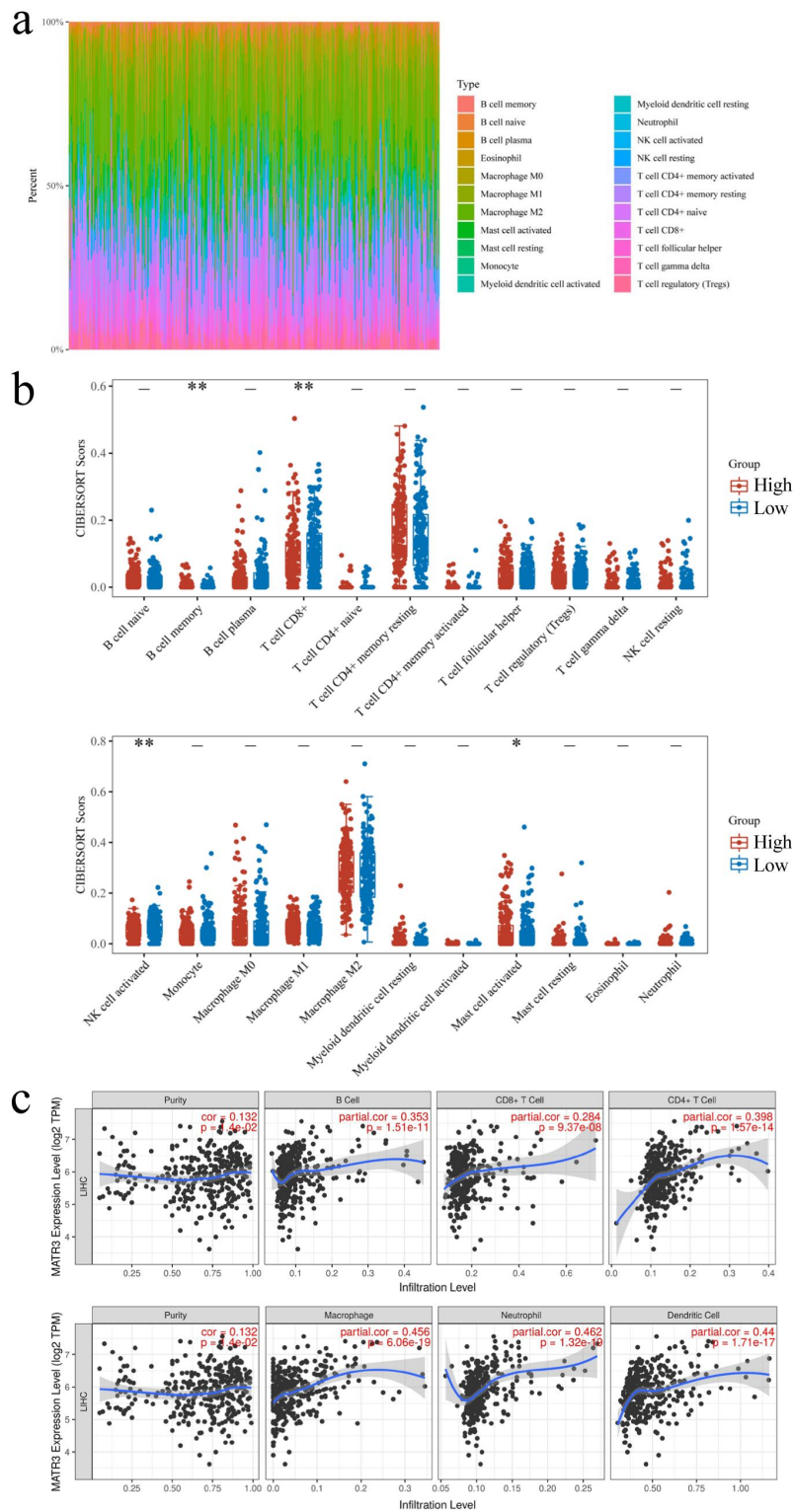
Figure 5. Relationship between MATR3 expression and immune cells.

(a) Infiltrating levels of 22 immune cells in HCC patients were analyzed by CIBERSORT. (b) The immune scores in HCC samples with high and low MATR3 expression. (c) Correlation between MATR3 expression and 6 types of immune cells in the TIMER database. ****$p < 0.0001$, ***$p < 0.001$, **$p < 0.01$, *$p < 0.05$, n.s, not significance. HCC, hepatocellular carcinoma.

Table 2. Correlation analysis between MATR3 and marker genes of immune cells in TIMER.

Description	Marker genes	None		Purity	
		Cor	P	Cor	P
CD8+ T cell	CD8A	0.152	**	0.255	****
	CD8B	0.06	0.247	0.149	**
	CD45(PTPRC)	0.461	****	0.604	****
T cell (general)	CD3D	0.029	0.573	0.117	*
	CD3E	0.107	*	0.232	****
	CD2	0.092	0.0772	0.209	****
B cell	CD19	0.139	**	0.186	***
	CD79A	0.074	0.155	0.165	**
	CD27	0.085	0.104	0.193	***
	CD20(KRT20)	0.173	***	0.181	***
Monocyte	CD14	−0.254	****	−0.242	****
	CD115 (CSF1R)	0.245	****	0.385	****
TAM	CCL2	0.169	**	0.276	****
	CD68	0.204	****	0.292	****
	IL10	0.26	****	0.372	****
M1 Macrophage	INOS (NOS2)	0.196	***	0.208	***
	CD80	0.361	****	0.478	****
	IRF5	0.42	****	0.414	****
	IL6	0.114	*	0.198	***
	CD64(FCGR1A)	0.169	**	0.292	****
M2 Macrophage	CD163	0.25	****	0.375	****
	CD206(MRC1)	0.097	0.0624	0.147	**
	VSIG4	0.181	***	0.297	****
	MS4A4A	0.208	****	0.342	****
Neutrophil	CD66B(CEACAM8)	0.059	0.256	0.08	0.137
	CD11B(ITGAM)	0.302	****	0.387	****
	CD15(FUT4)	0.443	****	0.48	****
Natural killer cell	KIR2DL1	0.021	0.691	0.007	0.899
	KIR2DL3	0.178	***	0.216	****
	KIR3DL1	0.164	**	0.196	***
	KIR3DL2	0.086	0.0964	0.145	**
	CD56(NCAM1)	0.324	****	0.394	****
	CD335(NCR1)	0.234	****	0.299	****
Dendritic cell	BDCA-1(CD1C)	0.243	****	0.326	****
	BDCA-4(NRP1)	0.613	****	0.651	****
	BDCA-3(CD14)	−0.254	****	−0.242	****
	CD123(IL3RA)	−0.011	0.831	−0.046	0.39
Th1	T-bet (TBX21)	0.114	*	0.204	***
	STAT4	0.162	**	0.216	****
	STAT1	0.503	****	0.555	****
Th2	GATA3	0.192	***	0.321	****
	STAT6	0.479	****	0.463	****
	IL13	0.089	0.0873	0.079	0.144
Tfh	BCL6	0.477	****	0.482	****
	IL21	0.111	*	0.143	**
Th17	STAT3	0.404	****	0.458	****
	IL17A	0.127	*	0.143	**
Treg	FOXP3	0.246	****	0.288	****
	CD25(IL2RA)	0.258	****	0.371	****
	CCR8	0.431	****	0.528	****
	STAT5B	0.696	****	0.691	****
T cell exhaustion	PD-1 (PDCD1)	0.146	**	0.222	****
	CTLA4	0.135	**	0.228	****
	LAG3	0.092	0.0756	0.131	*
	TIM-3 (HAVCR2)	0.261	****	0.403	****
	GZMB	0.068	0.193	0.117	*

TAM, tumor-associated macrophage; Th, T helper cell; Tfh, Follicular helper T cell; Treg, regulatory T cell; Cor, R value of Spearman's correlation; None, correlation without adjustment. Purity, correlation adjusted by purity. ****p < 0.0001, ***p < 0.001, **p < 0.01, *p < 0.05.

the markers of TAM, M2 macrophages and Treg (Table 3). These results indicate that MATR3 might play a vital role in immune infiltration in HCC.

Knocking down MATR3 inhibits tumor progression in vivo

Given the significant inhibition of HCC cell survival by the knockdown of MATR3 *in vitro*, we examined its activity *in vivo*. We employed a xenograft mouse model and injected the HepG2 cells into the nude mice in the control group and the MATR3 knockdown group. Consistent with the *in vitro* results, MATR3 silencing repressed tumor progression. The sizes and weights of the tumors in the shMATR3 group mice were significantly reduced compared with those in the shMATR3-control mice (Figure 6(a)–(c)). Immunohistochemistry analysis showed a predominant decrease in MATR3 expression in the tumor tissues of the MATR3 knockdown group, compared to that in the control group (Figure 6(d)). These findings suggest that MATR3 may regulate the tumorigenesis of HCC *in vivo*.

Discussion

HCC is the most common phenotype of liver cancer, characterized by high proliferation and metastasis [45]. Despite significant improvements in HCC diagnosis and treatment, the overall survival rate of HCC patients remains dismal. Therefore, it is of great significance to understand the molecular mechanism of HCC tumorigenesis. MATR3 is an abundant nuclear matrix protein that binds to DNA and RNA and regulates important biological functions [16,46,47]. Mutations in the coding region of MATR3 lead to amyotrophic lateral sclerosis and autosomal-dominant distal myopathy [17,48]. Importantly, MATR3 plays a role in chromatin structure and function [49]. Recent studies have documented the role of MATR3 in human cancers, with its dual function as both an oncogene and a tumor suppressor [26–28,50]. Nevertheless, the potential role of MATR3 in the oncogenesis of HCC remains skeptical.

In this study, we first performed an integrated computational analysis of the TCGA and GEO datasets and verified an elevated expression of MATR3 in HCC. The results of RT-qPCR and IHC staining also proved that the expression of

Table 3. Correlation analysis between MATR3 and T cells, B cell and macrophages markers in GEPIA.

Description	Marker genes	Tumor		Normal	
		R	P	R	P
CD8+ T cell	CD8A	0.3	*	0.096	0.066
	CD8B	0.15	**	0.33	*
	CD45	0.033	0.52	0.23	0.1
T cell (general)	CD3D	0.14	**	0.28	0.053
	CD3E	0.072	0.17	0.22	0.13
	CD2	0.1	*	0.17	0.25
B cell	CD19	0.019	0.71	0.11	0.44
	CD79A	0.031	0.55	0.16	0.26
	CD27	0.1	*	0.31	*
	CD20(KRT20)	0.019	0.71	−0.092	0.53
TAM	CD11B	0.16	**	0.23	0.11
	CD68	0.066	0.21	0.29	*
M1 Macrophage	INOS (NOS2)	−0.11	*	0.21	0.14
	COX2(PTGS2)	0.048	0.35	0.24	0.09
	IRF5	0.14	**	0.26	0.073
M2 Macrophage	CD163	0.15	**	0.17	0.23
	CD206(MRC1)	−0.064	0.22	0.078	0.59
Treg	FOXP3	−0.11	*	0.22	0.12
	CD25(IL2RA)	0.1	*	−0.054	0.71
	CCR8	−0.023	0.66	0.14	0.34
	STAT5B	−0.03	0.57	0.34	*
	TGFβ (TGFB1)	0.31	****	0.36	**

TAM, Tumor-associated macrophages; Treg, regulatory T cell. Tumor, correlation analysis in tumor tissue of TCGA. Normal, correlation analysis in normal tissue of TCGA. ****$p < 0.0001$, ***$p < 0.001$, **$p < 0.01$, *$p < 0.05$.
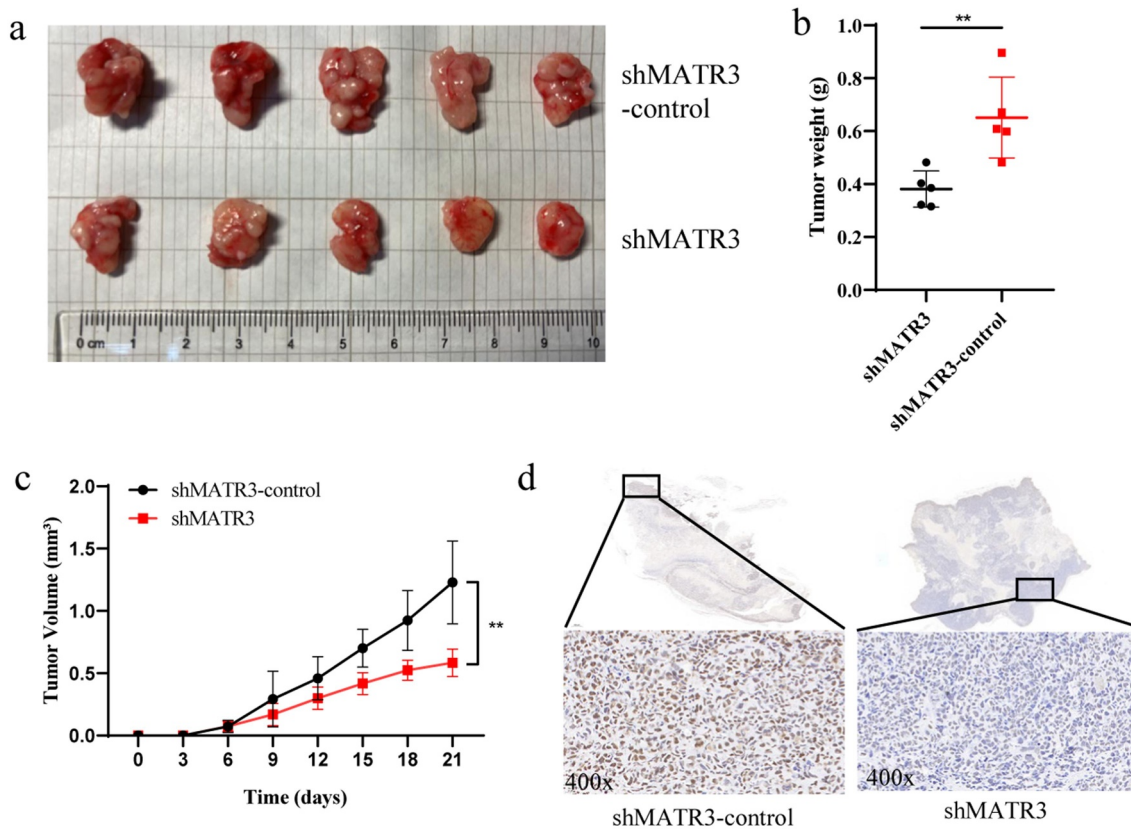
Figure 6. Knockdown of MATR3 inhibited cell growth of HCC *in vivo*.
(a) Macroscopic appearance of isolated tumors. (b-d) Tumor weight, tumor volume and immunohistochemistry analysis of MATR3 (magnification, 400 ×) in shMATR3 and control group of xenograft nude mice. ****$p < 0.0001$, ***$p < 0.001$, **$p < 0.01$, *$p < 0.05$, n.s, not significance.

MATR3 was significantly increased both in HCC cell lines and in human samples. Moreover, high MATR3 expression was also associated with clinicopathological features in HCC. Furthermore, ROC curves exhibited a promising diagnostic value for MATR3 in distinguishing HCC patients from healthy individuals. Meanwhile, we found that upregulated MATR3 was an important independent prognostic factor for the survival of HCC patients, which is consistent with a previous report that high MATR3 mRNA expression leads to a poor prognosis in patients with neuroblastoma [27]. Hence, our finding suggest that MATR3 can be used as a potential prognostic factor in HCC.

To gain mechanistic insights into how MATR3 contributes to the malignant transformation of HCC, we performed MATR3 co-expression gene enrichment analysis and found that MATR3 was significantly enriched in the processing of cell cycle-regulating pathways such as transcription (DNA-template) and mitotic cell cycle processes, and capped intron-containing pre-mRNA, In addition, our study revealed that knockdown of MATR3 inhibited HCC proliferation *in vitro*, and arrested the cell cycle, as revealed by the abundance of cells in the sub-G0/G1 stage as compared to fewer cells in the sub-S stage. Furthermore, we detected decreased mRNA levels of CDK6, CCND1 and CCND2, and increased mRNA expression of p21 and p27 after MATR3 knockdown. Cell cycle assessments showed that CCND1 and CCND2 could form active complexes with CDK6, which in turn phosphorylate the retinoblastoma protein and drive G1 to S phase progression [51]. This suggests that the accumulation phenomenon in the G0/G1 phase when MATR3 knockdown occurs in cells might be due to the suppression of CDK6, CCND1 and CCND2 levels. Nevertheless, p21 and p27, as Cip/Kip family members, could inhibit the kinase activities of

CDK6 to block the G1/S transition [52]. Therefore, we presumed that the upregulation of p21 and p27 might be another mechanism of G0/G1 phase arrest induced by MATR3 downregulation. We then screened the MATR3 interactome by Co-IP/MS and some of these proteins were found enriched in cell cycle-related pathways, such as S phase and G1/S transition, including STAG2 and PDS5A, which had been verified as the interaction partners of MATR3 [40]. MATR3 maintains chromatin structure by stabilizing the cohesin-CTCF protein complex in the chromatin and regulating gene expression during differentiation [49]. Cohesin is a ubiquitously expressed multiprotein complex and plays important roles in chromatid segregation, chromosome organization, gene expression, and DNA repair [53–56]. In vertebrate cells, the cohesin complex consists of four core subunit proteins: SMC1A, SMC3, RAD21, and either STAG1 or STAG2. Several additional subunits serve to regulate the core complex, including PDS5A, PDS5B, NIPBL, MAU2, WAPL, and sororin [57]. The cohesin subunits form a ring-shaped structure that encircles chromatin, which is loaded onto the chromatin in the early G1 phase of the cell cycle immediately following cytokinesis, concatenates sister chromatids during DNA replication in S phase, and releases from the chromatin at the early stage of mitosis [58,59]. The absence of STAG2 subunit causes disruption of cohesin interaction with the replication machinery, causing replication fork collapse, DNA double-strand breaks, and DNA damage checkpoint activation, ultimately resulting in intra-S-phase cell cycle arrest in primary human cells [60]. Moreover, PDS5A participates in replication fork protection and promotes DNA replication in the S phase [61]. Therefore, we speculate that MATR3, as an important cohesin-interacting protein, regulates DNA replication and cell cycle progression in S phase by interacting with STAG2 and PDS5A, and stabilizing the binding of cohesin to chromatin. These findings suggest that MATR3 forms an interactome with these cell-cycle regulating genes, and knocking down MATR3 may impede the cell cycle. All the above findings supported the cell cycle-regulating function of MATR3 in HCC.

Subsequently, we constructed a cell cycle-associated prognostic model based on the MATR3 protein interactome that comprised RFC2 and PRIM2. RFC2 modulates G1/S transition and promotes the proliferation by directly targeting miR-744 in colorectal cancer [62], PRIM2 that facilitate cell cycle and tumor progression in p53-mutant lung cancer [63], and regulator of chromatin condensation 1 that enhances G1/S progression via Cdk1 in cervical cancer cells [64]. Univariate COX analysis indicated that MATR3 and the prognostic model were prognostic factors of HCC. However, when they were put together for multivariate Cox analysis, they were not independent prognostic factors. Interestingly, when MATR3 and the model were separated and then conducted with other factors by multivariate Cox analysis respectively, they all showed independent prognostic significance. The possible reason was the existence of multicollinearity between the two covariates of MATR3 and the prognostic model in multivariate COX analysis. RFC2, PRIM2, and MATR3 may be the interacting proteins, and their expression may be affected by each other. Remarkably, the statistical significance of MATR3 was gerater than the prognostic model as an independent prognostic factor in HCC. Therefore, on the basis of MATR3 as a prognostic factor, this model might play an important role in improving the prediction accuracy of HCC patients as an auxiliary prognostic factor.

Increasing evidence has shown the role of the tumor microenvironment and TIICs in tumorigenesis and disease progression [65]. TAMs predominantly refer to a polarized M2 phenotype, expressing high levels of anti-inflammatory cytokines, which promote tumor progression by inhibiting the antitumor immune response mediated by T cells and reprograming the immunosuppressive microenvironment [66]. Tregs inhibit the antitumor activity of CD8$^+$ cytotoxic T lymphocytes and NK cells by directly interacting with them or producing immunoregulatory cytokines such as IL-10 and TGF-β [67]. As important immune suppressor cells, TAMs and Tregs play a regulatory role in tumor progression and predict poor prognosis in patients [68,69]. In our study, MATR3 was positively related to TAMs, M2

macrophages and Tregs in HCC. It is reported that cancer cells can suppress immune responses and promote tumor immune escapes by recruiting immunosuppressive cells and/or expressing immune checkpoint proteins [70]. Based on this evidence, it is plausible that overexpressed MATR3 may promote tumor immune escape and tumor progression by recruiting TAMs, M2 macrophages and Tregs and may affect the survival rate of patients by regulating the TIICs and tumor immune microenvironment in HCC.

However, the current study is limited. First, this study mainly employed the integrated bioinformatics analysis of the publicly available gene expression data and thus warrants further studies based on large number of clinical samples and animal experiments to gain mechanistic insights into the oncogenic function of MATR3 and its interacting partner proteins in HCC. Second, more specifically, there is a lack of description of the detailed mechanism employed by MATR3 to recruit TAMs, M2 macrophages, and Tregs, thus modulating the immune microenvironment. Nevertheless, it is worth mentioning that this study uncovers the novel oncogenic function of MATR3 in HCC. Further studies deciphering the molecular mechanism of MATR3 in the regulation of DNA replication and cell cycle would be excellent future research avenues in HCC carcinogenesis. To this end, future studies directed at understanding MATR3 function in cellular processes will likely lead to the discovery of novel functions and mechanisms, specifically in association with its interaction with RNA, DNA, and other proteins. Advancements in techniques such as CRISPR/Cas9-based gene editing will enable molecular pathways associated with MATR3 in HCC. Moreover, large-scale clinical studies containing large and diverse patient cohort would be needed to test the biomarker potentials of MATR3 in HCC. Furthermore, preclinical evaluation in vitro and in animal models are warranted to test the therapeutic potentials of MATR3. Importantly, these findings may guide MATR3-targeted therapy with standard treatment modalities.

This is the first study to uncover the upregulation and the clinical relevance of MATR3 in HCC. Overexpressed MATR3 predicted an unfavorable prognosis in HCC. Furthermore, MATR3 plays a vital role in regulating the immune microenvironment and cell cycle in HCC. In addition, a cell cycle-related prognosis model was constructed to predict the survival of HCC patients together with MATR3. Owing to its role in HCC progression, MATR3 may pave the way for the development of an effective biomarker and therapeutic strategy for HCC.

Abbreviations

MATR3	matrin-3;
HCC	hepatocellular carcinoma;
ICIs	immune checkpoint inhibitors;
NMPs	nuclear matrix proteins;
Co-IP/MS	co-immunoprecipitation and mass spectrometry;
TCGA-LIHC	Liver Hepatocellular Carcinoma Project of The Cancer Genome Atlas;
ICGC-LIRI-JP	Liver Cancer-RIKEN, Japan Project from International Cancer Genome Consortium;
GEO	Gene Expression Omnibus;
ROC	receiver operating characteristic;
KM	Kaplan-Meier;
PPI	protein-protein interaction;
AUC	area under curve;
PBS	phosphate buffered saline;
CCK-8	Cell Counting Kit-8;
CDK6	cyclin-dependent kinase 6;
CCND1	cyclin D1;
CCND2	cyclin D2;
p21	cyclin-dependent kinase inhibitor p21;
p27	cyclin-dependent kinase inhibitor p27;
CDK4	cyclin-dependent kinase 4;
CCNE1	cyclin E1;
TIICs	tumor-infiltrating immune cells;
TAM	tumor-associated macrophage;
RFC2	replication factor C 2;
PRIM2	DNA primase subunit 2

Consent to publish

All authors agreed to publish the article.

Credit Author Statement

Hengjing He and Muhammad Jamal: Investigation, Methodology, Validation, Formal analysis, Writing – original draft. Xingruo Zeng: Investigation, Resources. Yufei Lei: Investigation, Resources. Di Xiao: Investigation, Resources. Zimeng Wei: Investigation, Resources. Chengjie Zhang: Investigation, Resources. Xiaoyu Zhang: Investigation, Resources. Shan Pan: Investigation, Resources, Data curation. Qianshan Ding: Investigation, Resources, Data curation. Haiyan Tan: Conceptualization, Formal analysis, Resources. Songping Xie: Conceptualization, Formal analysis, Resources. Qiuping Zhang: Conceptualization, Investigation, Data curation, Funding acquisition, Project administration, Supervision, Writing – review & editing.

Data availability statement

All datasets used and analyzed during this study are available from the corresponding author on reasonable request.

Ethics approval

This study was performed in line with the principles of the Declaration of Helsinki. Approval was granted by the Ethics Committee of Renmin Hospital of Wuhan University.

References

[1] Villanueva A, Longo DL. Hepatocellular carcinoma. N Engl J Med. 2019;380(15):1450–1462. doi: 10.1056/NEJMra1713263

[2] Llovet JM, Kelley RK, Villanueva A, et al. Hepatocellular carcinoma. Nat Rev Dis Primers. 2021;7(1):6. doi: 10.1038/s41572-020-00240-3

[3] Sung H, Ferlay J, Siegel RL, et al. Global cancer statistics 2020: GLOBOCAN estimates of incidence and mortality worldwide for 36 cancers in 185 countries. CA Cancer J Clin. 2021;71(3):209–249. doi: 10.3322/caac.21660

[4] Huber TC, Bochnakova T, Koethe Y, et al. Percutaneous therapies for hepatocellular carcinoma: evolution of liver directed therapies. J Hepatocell Carcinoma. 2021;8:1181–1193. doi: 10.2147/JHC.S268300

[5] Koulouris A, Tsagkaris C, Spyrou V, et al. Hepatocellular carcinoma: an overview of the changing landscape of treatment options. J Hepatocell Carcinoma. 2021;8:387–401. doi: 10.2147/JHC.S300182

[6] Yuen MF, Cheng CC, Lauder IJ, et al. Early detection of hepatocellular carcinoma increases the chance of treatment: Hong Kong experience. Hepatology. 2000;31(2):330–335. doi: 10.1002/hep.510310211

[7] Slotta JE, Kollmar O, Ellenrieder V, et al. Hepatocellular carcinoma: Surgeon's view on latest findings and future perspectives. World J Hepatol. 2015;7(9):1168–1183. doi: 10.4254/wjh.v7.i9.1168

[8] Beretta L. Comparative analysis of the liver and plasma proteomes as a novel and powerful strategy for hepatocellular carcinoma biomarker discovery. Cancer Lett. 2009;286(1):134–139. doi: 10.1016/j.canlet.2009.01.025

[9] Rizzo A, Ricci AD, Di Federico A, et al. Predictive biomarkers for checkpoint inhibitor-based immunotherapy in hepatocellular carcinoma: where do we stand? Front Oncol. 2021;11:803133. doi: 10.3389/fonc.2021.803133

[10] Di Federico A, Rizzo A, Carloni R, et al. Atezolizumab-bevacizumab plus Y-90 TARE for the treatment of hepatocellular carcinoma: preclinical rationale and ongoing clinical trials. Expert Opin Investig Drugs. 2022;31(4):361–369. doi: 10.1080/13543784.2022.2009455

[11] Rizzo A, Cusmai A, Gadaleta-Caldarola G, et al. Which role for predictors of response to immune checkpoint inhibitors in hepatocellular carcinoma? Expert Rev Gastroenterol Hepatol. 2022;16(4):333–339. doi: 10.1080/17474124.2022.2064273

[12] Wan KM, Nickerson JA, Krockmalnic G, et al. The nuclear matrix prepared by amine modification. Proc Natl Acad Sci U S A. 1999;96(3):933–938. doi: 10.1073/pnas.96.3.933

[13] Gerner C, Gotzmann J, Fröhwein U, et al. Proteome analysis of nuclear matrix proteins during apoptotic chromatin condensation. Cell Death Differ. 2002;9(6):671–681. doi: 10.1038/sj.cdd.4401010

[14] Barboro P, Repaci E, D'Arrigo C, et al. The role of nuclear matrix proteins binding to matrix attachment regions (Mars) in prostate cancer cell differentiation. PLoS One. 2012;7(7):e40617. doi: 10.1371/journal.pone.0040617

[15] Durślewicz J, Klimaszewska-Wiśniewska A, Jóźwicki J, et al. Prognostic significance of MATR3 in stage I and II non-small cell lung cancer patients. J Cancer Res Clin Oncol. 2022;148(12):3313–3322. doi: 10.1007/s00432-022-04097-9

[16] Nakayasu H, Berezney R. Nuclear matrins: identification of the major nuclear matrix proteins. Proc Natl Acad Sci U S A. 1991;88(22):10312–10316. doi: 10.1073/pnas.88.22.10312

[17] Johnson JO, Pioro EP, Boehringer A, et al. Mutations in the Matrin 3 gene cause familial amyotrophic lateral sclerosis. Nat Neurosci. 2014;17(5):664–666. doi: 10.1038/nn.3688

[18] Salton M, Lerenthal Y, Wang S-Y, et al. Involvement of Matrin 3 and SFPQ/NONO in the DNA damage response. Cell Cycle. 2010;9(8):1568–1576. doi: 10.4161/cc.9.8.11298

[19] Zhang Z, Carmichael GG. The fate of dsRNA in the nucleus: a p54(nrb)-containing complex mediates the nuclear retention of promiscuously A-to-I edited RNAs. Cell. 2001;106(4):465–475. doi: 10.1016/S0092-8674(01)00466-4

[20] Attig J, Agostini F, Gooding C, et al. Heteromeric RNP Assembly at LINEs controls lineage-specific RNA processing. Cell. 2018;174(5):1067–1081.e17. doi: 10.1016/j.cell.2018.07.001

[21] Pollini D, Loffredo R, Maniscalco F, et al. Multilayer and MATR3-dependent regulation of mRnas maintains pluripotency in human induced pluripotent stem cells. iScience. 2021;24(3):102197. doi: 10.1016/j.isci.2021.102197

[22] Sarracino A, Gharu L, Kula A, et al. Posttranscriptional regulation of HIV-1 gene expression during replication and reactivation from latency by nuclear matrix protein MATR3. MBio. 2018;9(6). doi: 10.1128/mBio.02158-18

[23] Valencia CA, Ju W, Liu R. Matrin 3 is a Ca2+/calmodulin-binding protein cleaved by caspases. Biochem Biophys Res Commun. 2007;361(2):281–286. doi: 10.1016/j.bbrc.2007.06.156

[24] Sun J, Bai J, Jiang T, et al. Modulation of PDCD1 exon 3 splicing. RNA Biol. 2019;16(12):1794–1805. doi: 10.1080/15476286.2019.1659080

[25] Przygodzka P, Boncela J, Cierniewski CS. Matrin 3 as a key regulator of endothelial cell survival. Exp Cell Res. 2011;317(6):802–811. doi: 10.1016/j.yexcr.2010.12.009

[26] Kuriyama H, Fukushima S, Kimura T, et al. Matrin-3 plays an important role in cell cycle and apoptosis for survival in malignant melanoma. J Dermatol Sci. 2020;100(2):110–119. doi: 10.1016/j.jdermsci.2020.08.013

[27] Yang T-W, Sahu D, Chang Y-W, et al. RNA-Binding proteomics reveals MATR3 interacting with lncRNA SNHG1 to enhance neuroblastoma progression. J Proteome Res. 2019;18(1):406–416. doi: 10.1021/acs.jproteome.8b00693

[28] Chaudhary R, Gryder B, Woods WS, et al. Prosurvival long noncoding RNA PINCR regulates a subset of p53 targets in human colorectal cancer cells by binding to matrin 3. Elife. 2017;6:6. doi: 10.7554/eLife.23244

[29] Chandrashekar DS, Bashel B, Balasubramanya SAH, et al. UALCAN: a portal for facilitating tumor subgroup gene expression and survival analyses. Neoplasia. 2017;19(8):649–658. doi: 10.1016/j.neo.2017.05.002

[30] Vasaikar SV, Straub P, Wang J, et al. LinkedOmics: analyzing multi-omics data within and across 32 cancer types. Nucleic Acids Res. 2018;46(D1):D956–D963. doi: 10.1093/nar/gkx1090

[31] Zhou Y, Zhou B, Pache L, et al. Metascape provides a biologist-oriented resource for the analysis of systems-level datasets. Nat Commun. 2019;10(1):1523. doi: 10.1038/s41467-019-09234-6

[32] Szklarczyk D, Franceschini A, Wyder S, et al. STRING v10: protein-protein interaction networks, integrated over the tree of life. Nucleic Acids Res. 2015;43(Database issue):D447–D452. doi: 10.1093/nar/gku1003

[33] Shannon P, Markiel A, Ozier O, et al. Cytoscape: a software environment for integrated models of biomolecular interaction networks. Genome Res. 2003;13(11):2498–2504. doi: 10.1101/gr.1239303

[34] Tang Z, Li C, Kang B, et al. GEPIA: a web server for cancer and normal gene expression profiling and interactive analyses. Nucleic Acids Res. 2017;45(W1):W98–W102. doi: 10.1093/nar/gkx247

[35] Newman AM, Liu CL, Green MR, et al. Robust enumeration of cell subsets from tissue expression profiles. Nat Methods. 2015;12(5):453–457. doi: 10.1038/nmeth.3337

[36] Li T, Fan J, Wang B, et al. TIMER: a web server for comprehensive analysis of tumor-infiltrating immune cells. Cancer Res. 2017;77(21):e108–e110. doi: 10.1158/0008-5472.CAN-17-0307

[37] Hu G, Pen W, Wang M. TRIM14 promotes breast cancer cell proliferation by inhibiting apoptosis. Oncol Res. 2019;27(4):439–447. doi: 10.3727/096504018X15214994641786

[38] Huttlin EL, Bruckner RJ, Navarrete-Perea J, et al. Dual proteome-scale networks reveal cell-specific remodeling of the human interactome. Cell. 2021;184(11):3022–3040.e28. doi: 10.1016/j.cell.2021.04.011

[39] Iradi MCG, Triplett JC, Thomas JD, et al. Characterization of gene regulation and protein interaction networks for Matrin 3 encoding mutations linked to amyotrophic lateral sclerosis and myopathy. Sci Rep. 2018;8(1):4049. doi: 10.1038/s41598-018-21371-4

[40] Kim J-S, He X, Liu J, et al. Systematic proteomics of endogenous human cohesin reveals an interaction with diverse splicing factors and RNA-binding proteins required for mitotic progression. J Biol Chem. 2019;294(22):8760–8772. doi: 10.1074/jbc.RA119.007832

[41] Zhang X, Liu J, Yang X, et al. High expression of COL6A1 predicts poor prognosis and response to immunotherapy in bladder cancer. Cell Cycle. 2022;22(5):1–9. doi: 10.1080/15384101.2022.2154551

[42] Chen D, Zhang H, Zhao L, et al. Prognostic value of RILPL2 and its correlation with tumor immune microenvironment and glycolysis in non-small cell lung cancer. Cell Cycle. 2022;22(7):841–857. doi: 10.1080/15384101.2022.2159203

[43] Hirsch FR, Scagliotti GV, Mulshine JL, et al. Lung cancer: current therapies and new targeted treatments. Lancet. 2017;389(10066):299–311. doi: 10.1016/S0140-6736(16)30958-8

[44] Maibach F, Sadozai H, Seyed Jafari SM, et al. Tumor-infiltrating lymphocytes and their prognostic value in cutaneous melanoma. Front Immunol. 2020;11:2105. doi: 10.3389/fimmu.2020.02105

[45] Forner A, Reig M, Bruix J. Hepatocellular carcinoma. Lancet. 2018;391(10127):1301–1314. doi: 10.1016/S0140-6736(18)30010-2

[46] Zeitz MJ, Malyavantham KS, Seifert B, et al. Matrin 3: chromosomal distribution and protein interactions. J Cell Biochem. 2009;108(1):125–133. doi: 10.1002/jcb.22234

[47] Malyavantham KS, Bhattacharya S, Barbeitos M, et al. Identifying functional neighborhoods within the cell nucleus: proximity analysis of early S-phase replicating chromatin domains to sites of transcription, RNA polymerase II, HP1gamma, matrin 3 and SAF-A. J Cell Biochem. 2008;105(2):391–403. doi: 10.1002/jcb.21834

[48] Senderek J, Garvey SM, Krieger M, et al. Autosomal-dominant distal myopathy associated with a recurrent missense mutation in the gene encoding the nuclear matrix protein, matrin 3. Am J Hum Genet. 2009;84 (4):511–518. doi: 10.1016/j.ajhg.2009.03.006

[49] Cha HJ, Uyan Ö, Kai Y, et al. Inner nuclear protein Matrin-3 coordinates cell differentiation by stabilizing chromatin architecture. Nat Commun. 2021;12 (1):6241. doi: 10.1038/s41467-021-26574-4

[50] Nho S-H, Yoon G, Seo J-H, et al. Licochalcone H induces the apoptosis of human oral squamous cell carcinoma cells via regulation of matrin 3. Oncol Rep. 2019;41(1):333–340. doi: 10.3892/or.2018.6784

[51] Qie S, Diehl JA. Cyclin D1, cancer progression, and opportunities in cancer treatment. J Mol Med (Berl). 2016;94(12):1313–1326. doi: 10.1007/s00109-016-1475-3

[52] Yoon M-K, Mitrea DM, Ou L, et al. Cell cycle regulation by the intrinsically disordered proteins p21 and p27. Biochem Soc Trans. 2012;40(5):981–988. doi: 10.1042/BST20120092

[53] Michaelis C, Ciosk R, Nasmyth K. Cohesins: chromosomal proteins that prevent premature separation of sister chromatids. Cell. 1997;91(1):35–45. doi: 10.1016/S0092-8674(01)80007-6

[54] Guacci V, Koshland D, Strunnikov A. A direct link between sister chromatid cohesion and chromosome condensation revealed through the analysis of MCD1 in S. cerevisiae. Cell. 1997;91(1):47–57. doi: 10.1016/S0092-8674(01)80008-8

[55] Haarhuis JH, Elbatsh AM, Rowland BD. Cohesin and its regulation: on the logic of X-shaped chromosomes. Dev Cell. 2014;31(1):7–18. doi: 10.1016/j.devcel.2014.09.010

[56] Uhlmann F. SMC complexes: from DNA to chromosomes. Nat Rev Mol Cell Biol. 2016;17(7):399–412. doi: 10.1038/nrm.2016.30

[57] Morales C, Losada A. Establishing and dissolving cohesion during the vertebrate cell cycle. Curr Opin Cell Biol. 2018;52:51–57. doi: 10.1016/j.ceb.2018.01.010

[58] Canudas S, Smith S. Differential regulation of telomere and centromere cohesion by the Scc3 homologues SA1 and SA2, respectively, in human cells. J Cell Bio. 2009;187 (2):165–173. doi: 10.1083/jcb.200903096

[59] Remeseiro S, Cuadrado A, Carretero M, et al. Cohesin-SA1 deficiency drives aneuploidy and tumourigenesis in mice due to impaired replication of telomeres. EMBO J. 2012;31(9):2076–2089. doi: 10.1038/emboj.2012.11

[60] Mondal G, Stevers M, Goode B, et al. A requirement for STAG2 in replication fork progression creates a targetable synthetic lethality in cohesin-mutant cancers. Nat Commun. 2019;10(1):1686. doi: 10.1038/s41467-019-09659-z

[61] Morales C, Ruiz-Torres M, Rodríguez-Acebes S, et al. PDS5 proteins are required for proper cohesin dynamics and participate in replication fork protection. J Biol Chem. 2020;295(1):146–157. doi: 10.1074/jbc.RA119.011099

[62] Hu T, Shen H, Li J, et al. RFC2, a direct target of miR-744, modulates the cell cycle and promotes the proliferation of CRC cells. J Cell Physiol. 2020;235 (11):8319–8333. doi: 10.1002/jcp.29676

[63] Wang T, Tang T, Jiang Y, et al. PRIM2 promotes Cell cycle and tumor progression in p53-mutant lung cancer. Cancers (Basel). 2022;14(14):3370. doi: 10.3390/cancers14143370

[64] Qiao L, Zheng J, Tian Y, et al. Regulator of chromatin condensation 1 abrogates the G1 cell cycle checkpoint via Cdk1 in human papillomavirus E7-expressing epithelium and cervical cancer cells. Cell Death Dis. 2018;9(6):583. doi: 10.1038/s41419-018-0584-z

[65] Fu Y, Liu S, Zeng S, et al. From bench to bed: the tumor immune microenvironment and current immunotherapeutic strategies for hepatocellular carcinoma. J Exp Clin Cancer Res. 2019;38(1):396. doi: 10.1186/s13046-019-1396-4

[66] Yang L, Zhang Y. Tumor-associated macrophages: from basic research to clinical application. J Hematol Oncol. 2017;10(1):58. doi: 10.1186/s13045-017-0430-2

[67] Pitt JM, Marabelle A, Eggermont A, et al. Targeting the tumor microenvironment: removing obstruction to anticancer immune responses and immunotherapy. Ann Oncol. 2016;27(8):1482–1492. doi: 10.1093/annonc/mdw168

[68] Mantovani A, Marchesi F, Malesci A, et al. Tumour-associated macrophages as treatment targets in oncology. Nat Rev Clin Oncol. 2017;14(7):399–416. doi: 10.1038/nrclinonc.2016.217

[69] Ji D, Song C, Li Y, et al. Combination of radiotherapy and suppression of tregs enhances abscopal antitumor effect and inhibits metastasis in rectal cancer. J Immunother Cancer. 2020;8(2):e000826. doi: 10.1136/jitc-2020-000826

[70] Kitamura T, Qian B-Z, Pollard JW. Immune cell promotion of metastasis. Nat Rev Immunol. 2015;15(2):73–86. doi: 10.1038/nri3789